Enforcing Coherency in the Cluster of Grid-forming Inverters in Power Electronics-Dominated Grid

Muhammad F. Umar, *Student Member*, *IEEE*, Mohsen Hosseinzadehtaher, *Student Member*, *IEEE*,
Mohammad B. Shadmand, *Senior Member*, *IEEE*

Intelligent Power Electronics at Grid Edge (IPEG) Research Laboratory
Department of Electrical & Computer Engineering, University of Illinois Chicago
mumar6@uic.edu, mhosse5@uic.edu, shadmand@uic.edu

***Abstract*— This paper presents a control scheme for realization of coherency in a cluster of grid-forming inverters with heterogenous characteristics. Growing penetration of distributed generation (DG) leads the conventional grid towards more complex and disperse network known as power electronics dominated grid (PEDG). The complex structure of PEDG due to sparse nature requires an accurate model that can mimic the large-scale network dynamics. This will help to perform various analysis such as optimal coordination of controllers and real-time stability assessment. However, the inverters in PEDG have different parameters such as controller gains, filter parameters and power ratings. Thus, the inverters with heterogenous characteristics poses a challenge in obtaining accurate aggregate model of the PEDG. To enforce the homogeneity in the inverter's dynamic response, this paper proposes a coherency enforcement scheme that will shape the dynamic frequency response such that inverters with heterogenous characteristics behave coherently under various disturbances. Moreover, this will aid in deriving the accurate aggregate model of the PEDG. Several case studies under different disturbances are presented to validate the proposed coherency enforcement control. Furthermore, an aggregated model for grid-forming inverter after enforcing coherency is developed and dynamic response of the model is compared with actual circuit model.**

Keywords— grid-forming inverter, PEDG, virtual inertia, heterogenous DERs, aggregated model, homogeneous dynamic response

I. Introduction

Nowadays power system is transitioning from the central generation to more distributed generation to incorporate the renewable energy such as windfarms, solar PVs, etc. This transition leads to a new concept of power system known as power electronics dominated grid (PEDG) [1]. PEDG integrates renewable energy and creates flexible generation sources. However, the sparse and distributed nature of PEDG make the power system complex network [2-4]. Accurate dynamic models can help in predicting the dynamic response of such massive and distributive natured PEDG. Moreover, analyzing PEDG becomes less complex by representing an accurate aggregated model. However, the accuracy of the model highly depends on homogeneity of the inverter based distributed generation (DG) [5, 6]. Specifically, if the dynamic response of the inverters is similar then PEDG can be represented with an aggregated model with high accuracy.

The aggregation methods based on coherency to derive the accurate model of the non-linear synchronous machines are enabling scheme to perform various analysis such as economic dispatch and optimization on the power system [7]. The physical boundaries of the power system can be identified by leveraging the coherency identification scheme. The generation sources with similar voltage angle and frequency dynamic response to the disturbances are known as coherent generation sources [8, 9]. Furthermore, applying aggregation schemes on the coherent generation sources becomes much simpler and computationally efficient. Moreover, the coherent behaving generators can be clustered to form an accurate-aggregated model.

The methods for identification of coherency and aggregation of large-order system can effectively be used to preserve the model dynamics. Useful information can be extracted from the aggregated models of the large-order power system. Current aggregation and coherency detection methodologies can be divided under two types, (i) model based, and (ii) signal-based methodologies. In signal-based approaches the signals generated via wide-area monitoring devices such synchrophasors are used to extract the information of the power system to detect the coherency between generating sources. The benefits of the signal-based schemes includes fast identification and low dependence on the model-related data [10]. However, the signals from the wide-area monitoring devices are prone to disturbance and infiltration of malicious data [11].

Coherency identification and aggregation schemes based on the model are devised by altering the swing equation of the synchronous generation source to detect coherent cluster. Then, based on various model-reduction methodologies the order of the cluster is reduced [12]. The early work on the model reduction and coherency detection was carried out in 1980s and 1990s [7, 13]. The authors in [14] uses eigenvalue analysis to detect the coherent generation sources. Then, the large-order power system is partitioned into different cluster based on the coherency information. To achieve high accuracy from the proposed scheme it requires very precise information of the parameters and the model. Nevertheless, in many cases retrieving the full information about the model is not possible. In [15], slow-coherency scheme is applied for the clustering the generators by utilizing the DYNRED software. However, the presented analysis is valid for the specific equilibrium point and

978-1-6654-3635-9/21/$31.00 ©2021 IEEE

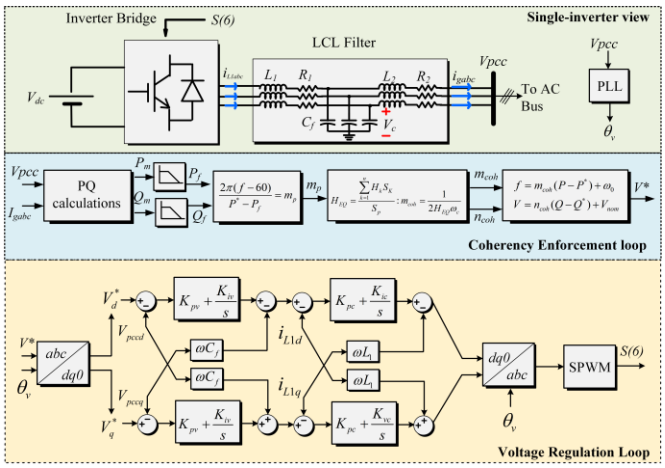

Fig. 1. Proposed controller architecture.

suffers from modeling imperfections, parametric uncertainties, and heterogenous network like PEDG.

The inverters form a major part of power generation mix in PEDG. Therefore, the coherency concepts from the power system can be applied to the inverter-based DGs to detect coherent cluster boundaries and achieve reduced-order model. In the existing literature, limited schemes are presented to address the coherency identification and developing aggregated models. For example, in [16] the differential geometry concept is applied to network of inverters to determine coherency in the frequency dynamic response but applying proposed scheme on such large network is complicated and required extensive validation and analysis. In [17], coherent equivalence method for modular multilevel inverters (MMI) equipped with virtual synchronous generator (VSG) control is presented. In this scheme the virtual power angles of the VSG-based MMI are exploited to identify the coherent behaving inverters. The developed equivalent model can mimic the dynamic response of the parallel VSG-controlled MMIs with limited accuracy. Nevertheless, a universal and generalized coherency identification scheme for the inverters is still unexplored in the literature. The coherency identification scheme based on the eigenvalue perturbation for droop controlled grid-forming inverter in a feeder is presented in [5]. However, each inverter can have different filter model parameters, controller gain and power ratings. The work in [5] considers all inverter's have similar physical parameters. Therefore, the dynamic response to the disturbance in inverters with dissimilar physical characteristics would not be homogenous and conclusively non-coherent dynamic response.

This paper proposes a coherency enforcement control based on autonomously deriving the equivalent inertia of a grid cluster by inverter's primary layer droop controller gains to realize an accurate aggregate model. The condition for coherency in the grid-forming inverters dictates that if the frequency or voltage angle dynamics after the disturbance such as load increase or decrease is similar for all connected inverters in a cluster then that cluster of inverters can be called coherent. The main contribution of the work is aggregation of network of grid-forming inverters having different physical characteristic such as filter parameters, control gains and inverter power ratings. This makes the proposed control scheme for aggregation more realistic as most of the inverters integrated in a modern-day grid are distinct. For instance, these have different manufacturer and depending on that different type of controllers and filter parameters. The developed coherency among the inverters in PEDG enables an accurate and comprehensive dynamic model development. The developed aggregated dynamic model is compared with the actual circuit model of the grid-forming inverters. The developed aggregated dynamic model accurately depicts the system dynamics under the load disturbances. Therefore, this work encompasses the unexplored domain in literature.

The rest of the paper is structured as follows: section II presents the formulation and validation of the proposed control coherency enforcement scheme. Then, mathematical modeling for the dynamic model of grid-forming inverter is discussed in section III. Simulation results of developed aggregated model tested under various loading conditions are discussed and compared with circuit-based model of grid-forming inverter in section IV. Finally, the conclusion of the work is presented in section V.

II. Proposed Coherency Enforcement Control Analysis

The proposed coherency enforcement control scheme is illustrated in Fig. 1. It should be remarked that the degree of coupling between the voltage and real power are assumed to be minimal, hence the well-known decoupled control rule is deployed in the proposed grid forming control architecture for each individual DG and is given by,

$$f - f_{ref} = \frac{m_p}{2\pi}(p_{ref} - P_f) \tag{1}$$

$$V - V_{ref} = n_q(Q_{ref} - Q_f) \tag{2}$$

where, f_{ref} and p_{ref} are the frequency and active power set points which are defined by the secondary layer of the control. f is the real time system frequency that can be matched to the converter's output frequency. In active power control equation, the filtered value of the power is used and denoted as P_f and the m_p is defined as the droop gain for the active power control. V_{ref} and Q_{ref} are nominal output voltage and nominal reactive power. V is the RMS value of the point of common coupling (PCC) voltage. Q_f is the calculated reactive power after low-pass filter and n_q is the droop gain for the reactive power control. To eliminate the low-order variation in the calculated powers, a low-pass filter is used in this methodology [19]. The mathematical relation of calculated active and reactive power and after passing via low-pass filter is given by,

$$P_f = \frac{P_m\,\omega_c}{\omega_c + s} \tag{3}$$

$$Q_f = \frac{Q_m\,\omega_c}{\omega_c + s} \tag{4}$$

ω_c is the cutoff frequency and P_m and Q_m is the measured active power and reactive power respectively. To attain the fundamental equation that describes virtual inertia emulation technique, the swing equation is used as the core of all virtual

inertia emulation approaches. Generally, this equation is demonstrated in per unit system, which is given by,

$$\frac{P_m - P_{ref}}{2\pi D_k} + \frac{4H\pi f}{D_k} f' = (f - f_{ref}) \tag{5}$$

$$\frac{s(f - f_{ref})}{\omega_c D_k} + \frac{f - f_{ref}}{D_k} = \frac{s\, p_{ref}}{2\pi\omega_c} - \frac{P_m - p_{ref}}{2\pi} \tag{6}$$

where H is defined as the inertia constant, D_k denotes the damping constant and f' is the rate of change of frequency (ROCOF). Analyzing (5) and (1) reveals that these equations are related by the change in frequency. Specifically, if frequency deviation from the nominal value is small and frequency and power setpoints remain constant, (5) and (1) can be combined and given by (6). Assuming the frequency deviation is under normal range and the right-hand side of (6) is approximately equal to zero. Then relation between inertia constant (H) and droop gain (m_p) is given as,

$$m_p = \frac{1}{2H\omega_c} \;;\; D_k m_p = 1 \tag{7}$$

The equivalent inertia constant of the entire cluster is calculated, firstly by evaluating the individual inertia constants of the inverters participating in virtual inertia emulation by (7). Then based on the rated power of each inverter and total power delivered in the cluster. The equivalent inertia is given by,

$$H_{EQ} = \frac{\sum_{k=1}^{n} H_k S_K}{S_p} = \frac{1}{S_p} \sum_{k=1}^{n} \frac{S_k}{2m_{p,k}\,\omega_c} \tag{8}$$

where, H_{EQ} is the equivalent inertia of the system, H_k is the individual inertia of the inverter, S_k , S_p are the nominal power of k_{th} inverters-based DG and the under-study power system, respectively, and n denotes the number of inverters connected in PEDG with emulated virtual inertia. It should be noted that the equivalent inertia is highly dependent on the individual apparent power of the inverter and the rated power of the energy grid. Furthermore, the voltage reference generated by the coherency enforcement loop is regulated by leveraging the voltage regulation loop depicted in the Fig. 1.

A. *Validation of Coherency enforcement in the cluster of grid-forming inverters*

The proposed coherency enforcement control scheme is validated for the cluster based on three DGs. The system parameters are specified in the Table I. Each of DGs in the cluster have different filter parameters, power ratings and controller gains as mentioned in the Table I. The extinct of enforced coherency between the DGs is tested. Firstly, disturbance in terms of 50 % load increase is introduced at instant t_1. Fig. 2 (a) depicts the formation of the system without proposed scheme in which all the DGs are disconnected as the circuit breakers between the DGs are open. The dynamic frequency response under this disturbance for non-coherent DGs is illusrated by Fig. 2 (b). Intutively, with hetergenous characteristics all DGs have distinct frequency response. Furthermore, another disturbance with 50 % load increase is introduced at instant t_2. Fig. 2 (c) depicts that without proposed

TABLE I: SYSTEM SPECIFICATIONS

Parameter	Value
DC Link Voltages V_{dc}	600 V
Sampling Time T_s	10 µs
Inverter-side Inductor L_{11}, L_{12}, L_{13}	1.4 mH, 1.6 mH, 1.2 mH
Grid-side Inductor L_{21}, L_{22}, L_{23}	0.35mH, 0.45mH, 0.25mH
Filter Capacitance C_{f1}, C_{f2}, C_{f3}	75 µF, 70 µF, 80 µF
Inductor Resistance R_1, R_2	0.1 Ω
Cut-off frequency ω_c	100 rad s^{-1}
Inverter rated power S_1, S_2, S_3	6,8,10 KVA
Inverter droop gains m_1, m_2, m_3	(2.5,3.5,5.5) x 10^{-4} s^{-1}

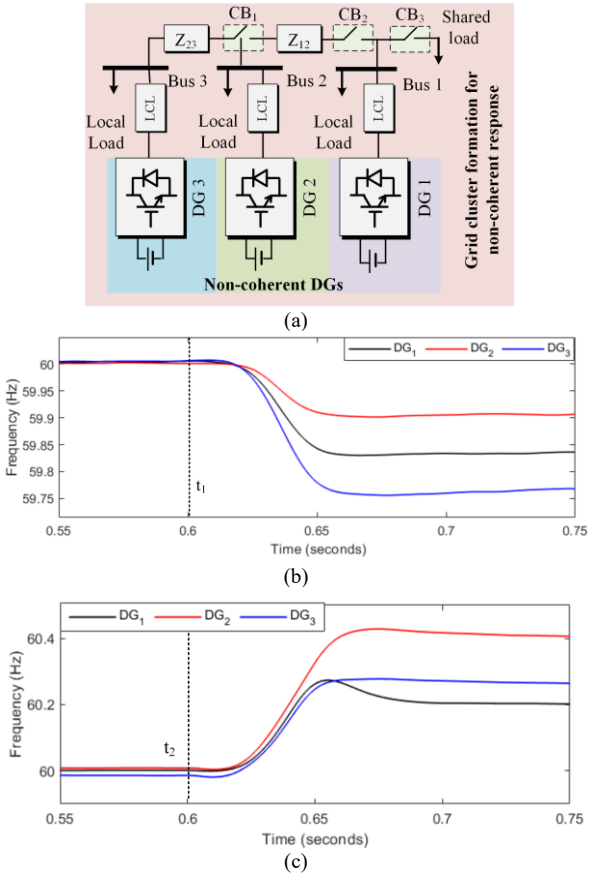

Fig. 2. Frequency dynamic response of the grid cluster without proposed control: (a) system configuration for desired dynamic response (b) frequency response of DGs with 50 % load increase, (c) frequency response of DGs 50 % load decrease.

control all DGs have dissmilar frequency dynamic response as each DG's follows different frequency transients.

Fig. 3 (a) depicts the configuration of the cluster with the proposed coherency enforcement control. Likewise to previous case, all the DGs are disconnected by opening the circuit breakers between the DGs. Although each DG has heterogenous characteristics but with proposed control the frequency dynamic response is homogenous under both load disturbances. Fig. 3 (b) and (c) validates that in both scenario of 50 % load increase and 50 % load decrease at instant t_1 and t_2, the frequency tranisents for all DGs are similar and thus behaving coherently.

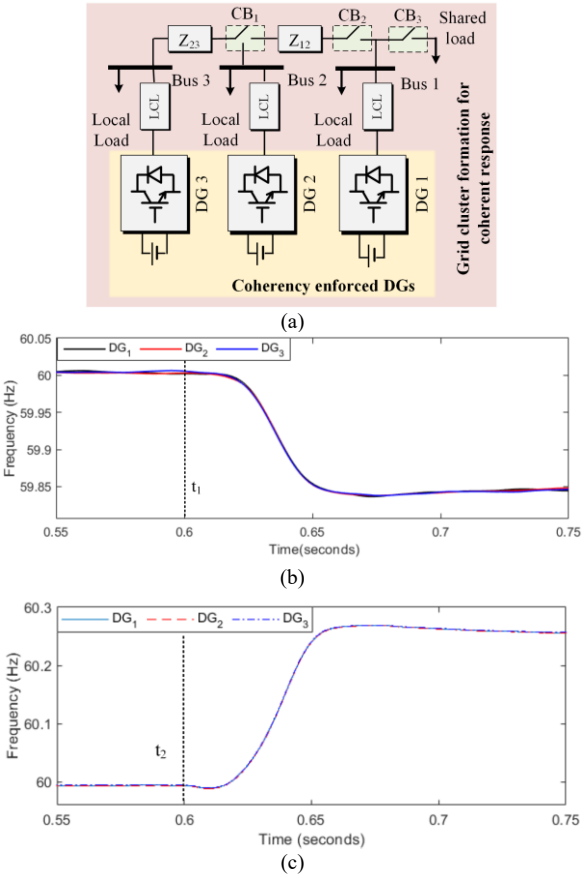

Fig. 3. Frequency dynamic response of the grid cluster with proposed coherency enforcement control: (a) system configuration for desired dynamic response (b) frequency response of DGs with 50 % load increase, (c) frequency response of DGs 50 % load decrease.

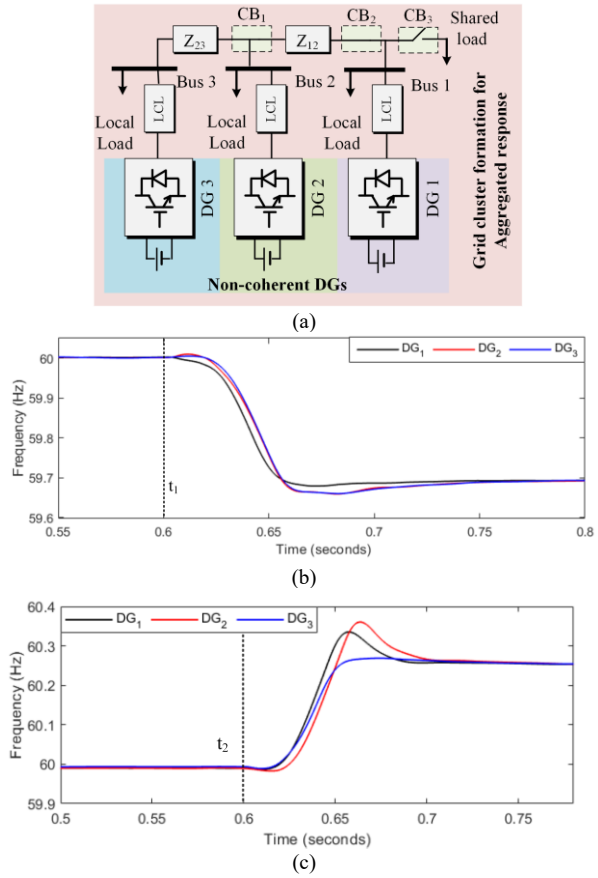

Fig. 4. Frequency dynamic response of the grid cluster of aggregated system formation: (a) system configuration for desired dynamic response (b) frequency response of DGs with 50 % load increase, (c) frequency response of DGs 50 % load decrease.

Further validation of the results generated from the proposed scheme is performed by comparing them with the aggregated response of all three DGs under the similar load disturbances. Specifically, Fig. 4 (a) depicts the cluster configuration to determine the aggregated response from all DGs. The circuit breakers between the DGs are connected to derive the aggregated frequency dynamic response. Fig. 4 (a) and (b) confirms that the aggregated frequency dynamic response of the cluster is similar to the frequency dynamic response obtained from the each DGs with proposed coherency enforcement control. Particularly, the steady-state frequency values of the DGs with the proposed control and aggregated response matches before and after the load distrubances. Therefore, this verifies that after enforcing coherency between the DGs with hetergoenous characteristics all three DGs can be represented as single and aggregated model.

III. Dynamic Model of Grid-Forming Inverter

After enforcing the coherency in the PEDG having inverters with heterogenous characteristics, the accurate model of the system is formulated mathematically, and then dynamic response of the model is compared with the circuit model depicted in Fig. 1 and PEDG in Fig. 2. The comprehensive mathematical model of the grid-forming inverter comprised of fourteen states. Therefore, modelling the dynamics in the active power, reactive power and voltage angle, the state-space equations are given by,

$$\theta = \omega_0 t - m_p \int (P_f - P^*) dt \tag{9}$$

$$V^*_{pccd} = V_{pccd} - n(Q_f - Q^*) \tag{10}$$

Moreover, the derived state-space model[20] by leveraging (9) and (10) is given as,

$$\begin{bmatrix} \dot{\theta} \\ \dot{P} \\ \dot{Q} \end{bmatrix} = A_1 \begin{bmatrix} \theta \\ P \\ Q \end{bmatrix} + B_1 \begin{bmatrix} i_{1dq} \\ V_{pccdq} \\ i_{gdq} \end{bmatrix} + B_2[\omega_c] \tag{11}$$

where,

$$A_1 = \begin{bmatrix} 0 & -m_{coh} & 0 \\ 0 & -\omega_c & 0 \\ 0 & 0 & -\omega_c \end{bmatrix}, \; B_1 = \begin{bmatrix} 0 & 0 & 0 & 0 & 0 & 0 \\ 0 & 0 & 3\omega_c i_{gd} & 3\omega_c i_{gq} & 3\omega_c v_{pccd} & 3\omega_c v_{pccq} \\ 0 & 0 & \omega_c i_{gq} & \omega_c i_{gd} & -\omega_c v_{pccq} & -\omega_c v_{pccd} \end{bmatrix}$$

$$B_2 = [-1 \quad 0 \quad 0]^T$$

where θ corresponds to the voltage angle, i_{gd} and i_{dq} are the d-q compoents of the output current, v_{pccd} and v_{pccq} are the d-q componets of the point of common coupling voltage, m_{coh} is the modified droop gain from the coherency enforcement control, and ω_c is the cut-off frequency of the low-pass filter.

The dynamics in the point of common coupling voltage, output current and inveter side current are modeled by firstly

writing the dynamic equations for each variable and then deriving the state-space model. The dynamic equations for each parameter in d-q reference frame is given by,

$$\frac{di_{1d}}{dt} = -\frac{R_1}{L_1} i_{1d} + \omega i_{1q} + \frac{1}{L_f}(v_{invd} - v_{cd}) \tag{12}$$

$$\frac{di_{1q}}{dt} = -\frac{R_1}{L_1} i_{1q} + \omega i_{1d} + \frac{1}{L_f}(v_{invq} - v_{cq}) \tag{13}$$

$$\frac{dv_{cd}}{dt} = \omega v_{cd} + \frac{1}{C_f}(i_{1d} - i_{gd}) \tag{14}$$

$$\frac{dv_{cq}}{dt} = -\omega v_{cq} + \frac{1}{C_f}(i_{1q} - i_{gq}) \tag{15}$$

$$\frac{di_{gd}}{dt} = \frac{-R_1 - R_2}{L_1 + L_2} i_{gd} + \omega i_{gq} + \frac{1}{L_1 + L_2}(v_{cd} - v_{pccd}) \tag{16}$$

$$\frac{di_{gq}}{dt} = \frac{-R_1 - R_2}{L_1 + L_2} i_{gq} - \omega i_{gd} + \frac{1}{L_1 + L_2}(v_{cq} - v_{pccq}) \tag{17}$$

The state-space model for the above-mentioned dynamic equations is given by,

$$\begin{bmatrix} \dot{i}_{1-dq} \\ \dot{v}_{c-dq} \\ \dot{i}_{g-dq} \end{bmatrix} = A_2 \begin{bmatrix} i_{1-dq} \\ v_{c-dq} \\ i_{g-dq} \end{bmatrix} + B_3 \begin{bmatrix} v_{inv-dq} \end{bmatrix} + B_4[\theta] + B_5[\omega] \tag{18}$$

where,

$$A_1 = \begin{bmatrix} \frac{R_1}{L_1} & \omega & \frac{-1}{L_1} & 0 & 0 & 0 \\ -\omega & \frac{-R_1}{L_1} & 0 & \frac{-1}{L_1} & 0 & 0 \\ \frac{1}{C_f} & 0 & 0 & \omega & \frac{-1}{C_f} & 0 \\ 0 & \frac{1}{C_f} & -\omega & 0 & 0 & \frac{-1}{C_f} \\ 0 & 0 & \frac{-1}{L_1 + L_2} & 0 & \frac{-R_1 - R_2}{L_1 + L_2} & \omega \\ 0 & 0 & 0 & \frac{1}{L_1 + L_2} & -\omega & \frac{-R_1 - R_2}{L_1 + L_2} \end{bmatrix}, B_3 \begin{bmatrix} \frac{1}{L_1} & 0 \\ 0 & \frac{1}{L_1} \\ 0 & 0 \\ 0 & 0 \\ 0 & 0 \\ 0 & 0 \end{bmatrix}$$

$$B_4 = \begin{bmatrix} 0 & 0 & 0 & 0 & \frac{v_{pcc} \sin\theta_v}{L_1 + L_2} & \frac{-v_{pcc} \cos\theta_v}{L_1 + L_2} \end{bmatrix}^T$$

$$B_5 = \begin{bmatrix} i_{1q0} & -i_{1d0} & v_{cq0} & -v_{cd0} & i_{gq0} & -i_{gd0} \end{bmatrix}^T$$

where, v_{cd} and v_{cq} are the filter capacitor voltage d-q components, v_{invd} and v_{inq} is the d-q components of the bridge voltage. Moreover, the matrix B_5 contains initial values of the various parameters of the model. These initial values are given in the Table II.

IV. Results and Discussion

The state-space model developed in the previous section is perturbed with the step change in the active power. The initial conditions of the states in the model are given in Table II.

TABLE II: Initial Conditions

Parameter	Value
Voltage angle θ_{v0}	2.02 rad/s
Active power P_0	50 W
Reactive power Q_0	0 VARs
Inverter-side current i_{1d0}, i_{1q0}	0.737 A, 0.02 A
Output current i_{gd0}, i_{gq0}	0.430 A, 0.015 A
Filter capacitor voltage v_{cd0}, v_{cq0}	122 V, 0 V
Point of common coupling voltage v_{pccd0}, v_{pccq0}	120 V, 0 V

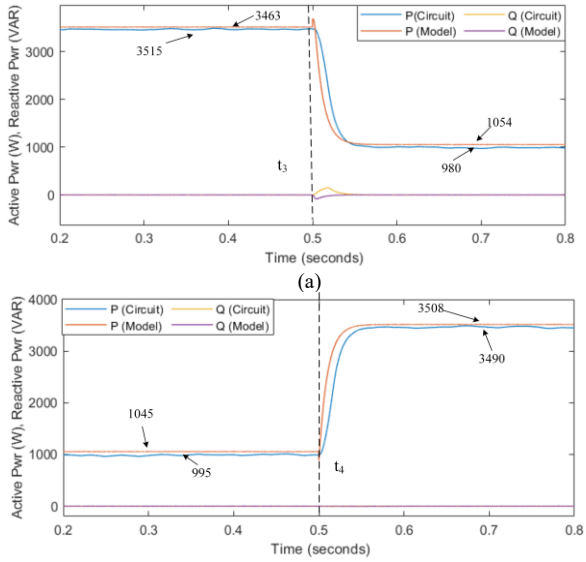

Fig. 5. Active and reactive power dynamic response of model and ciruit of grid-forming inverter: (a) negative step change in active power , (b) positive step change in active power.

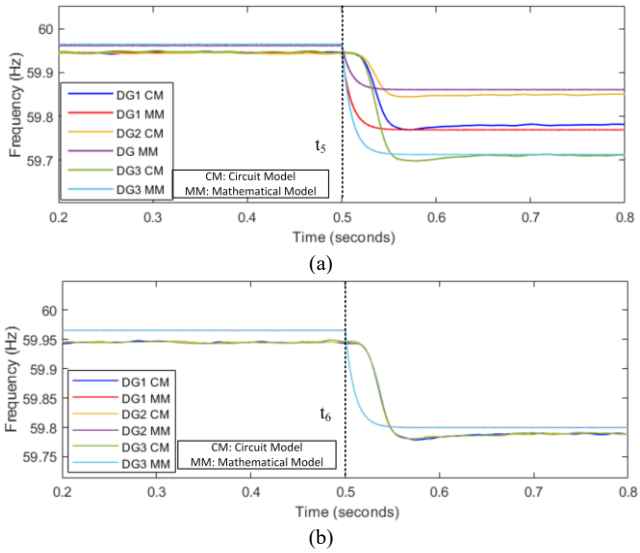

Fig. 6. Frequency dynamic response of model and ciruit of grid-forming inverter: (a) without proposed control, (b) with proposed coherency enforcement control.

Moreover, the dynamic response of the model is compared with the actual circuit model of the grid-forming inverter to validate the proposed control. Fig. 5 (a) depicts the active power dynamic response of the model of grid-forming inverter as

compared to the actual circuit model of the grid-forming inverter. At instant t_3 the load on Bus 1 was reduced and the active power injected was reduced from 3500 W to 1000 W. The active power from both mathematical model and circuit model of the grid-forming inverter illustrates similar dynamics. There is a small steady-state error between the active power values from the mathematical model and circuit model of the grid-forming inverter. For instance, when actual circuit model of the grid-forming inverter was supplying 3463 W, the active power output from the model was measured to be 3515 W. Moreover, after t_3 the active power supplied from the circuit is calculated as 980 W and from mathematical model it was calculated as 1054 W. This difference arises due to the various non-idealities in the circuit model of the grid-forming inverter such as switching losses, conduction losses, core losses, etc. Furthermore, at instant t_3 minimal change in reactive power from the circuit and model of grid-forming inverter was observed. Before and after t_3 the reactive power injection remain zero. Fig. 5(b) illustrates the active power dynamic response of the mathematical model and circuit of the grid-forming inverter to the positive step change in active power. Like previous case study, the active power dynamics of the grid-forming inverter are same. However, before and after t_4 there is a small steady-state error i.e., 50 W before t_4 and 18 W after t_4. Thus, this validates that mathematical model based on the coherency enforcement can accurately mimic the dynamics of the PEDG.

Moreover, the developed mathematical model is tested to determine the frequency dynamic response with and without the proposed control. Fig. 6 (a) illustrates the frequency dynamic response for the circuit model and mathematical model. It is inferred from the figure that without the proposed control all DGs have dissimilar frequency transients under the load disturbance. The developed mathematical model captures the dynamics in the frequency response matches to the circuit model of each DG with high accuracy. Fig. 6 (b) depicts the frequency transients under the load disturbance with the proposed control. Similarly, the developed mathematical model when compared with circuit model it captures the transients in frequency and all DGs have similar frequency dynamic response due to the proposed coherency control. Therefore, this validates the accuracy of developed mathematical model. Moreover, this concludes that it can be effectively used in conjunction with the proposed coherency control to represent the cluster of three DGs as a single aggregated model.

V. Conclusion

This paper presented a control scheme for enforcing coherency in a cluster of grid-forming inverters with heterogenous characteristics. Increasing penetration of distributed generation (DG) leads the conventional grid towards more complex and denser structure. Thus, it become more challenging to optimize and perform various analysis on large-scale networks. The aggregated and reduced-order models that accurately represent the PEDG enables various analysis such optimal coordination of controllers and stability analysis. However, the dissimilar characteristics of the inverter based DGs due to the different filter model parameters, inverter ratings and control algorithms poses a challenge to derive the aggregated model. In various case studies presented in the paper it was concluded with proposed control the non-coherent cluster of inverters can be coherent under various disturbances that includes load increase or load decrease. Finally, the circuit model of grid forming inverter and the model developed based on coherency enforcement control is compared. This comparison verified that the model mimics the dynamics of PEDG with high accuracy. Moreover, in this work a highly accurate mathematical model of the grid-forming inverter is presented. That can be utilized to represent the system dynamics of the grid cluster with a simplified and aggregated model if it is used in conjunction with coherency enforcement control.

Acknowledgment

This work was supported by the U.S. National Science Foundation under Grant ECCS-2114442. The statements made herein are solely the responsibility of the author.

Refrences

[1] A. Khan, M. Hosseinzadehtaher, M. B. Shadmand, S. Bayhan, and H. Abu-Rub, "On the Stability of the Power Electronics-Dominated Grid: A New Energy Paradigm," *IEEE Industrial Electronics Magazine,* vol. 14, no. 4, pp. 65-78, 2020, doi: 10.1109/MIE.2020.3002523.

[2] O. H. Abu-Rub, A. Y. Fard, M. F. Umar, M. Hosseinzadehtaher, and M. B. Shadmands, "Towards Intelligent Power Electronics-Dominated Grid via Machine Learning Techniques," *IEEE Power Electronics Magazine,* vol. 8, no. 1, pp. 28-38, 2021.

[3] Y. Gu, N. Bottrell, and T. C. Green, "Reduced-order models for representing converters in power system studies," *IEEE Transactions on Power Electronics,* vol. 33, no. 4, pp. 3644-3654, 2017.

[4] M. S. Ali, M. K. Ahmad, M. F. Umar, and S. M. R. Kazmi, "Comparison of non-isolated converter topologies for maximization of energy yield of photovoltaic energy conversion system," in *2018 1st International Conference on Power, Energy and Smart Grid (ICPESG)*, 2018: IEEE, pp. 1-6.

[5] P. J. Hart, R. H. Lasseter, and T. M. Jahns, "Coherency identification and aggregation in grid-forming droop-controlled inverter networks," *IEEE Transactions on Industry Applications,* vol. 55, no. 3, pp. 2219-2231, 2019.

[6] B. Nun, M. F. Umar, A. Karaki, M. B. Shadmand, S. Bayhan, and H. Abu-Rub, "Model Predictive Control for Black Start of Connected Communities via Autonomous Indexing," in *2021 IEEE 12th International Symposium on Power Electronics for Distributed Generation Systems (PEDG)*, 2021: IEEE, pp. 1-7.

[7] J. H. Chow, R. Galarza, P. Accari, and W. W. Price, "Inertial and slow coherency aggregation algorithms for power system dynamic model reduction," *IEEE Transactions on Power Systems,* vol. 10, no. 2, pp. 680-685, 1995.

[8] R. Podmore, "Identification of coherent generators for dynamic equivalents," *IEEE Transactions on Power Apparatus and Systems,* no. 4, pp. 1344-1354, 1978.

[9] X. Wang, V. Vittal, and G. T. Heydt, "Tracing generator coherency indices using the continuation method: A novel approach," *IEEE Transactions on Power Systems,* vol. 20, no. 3, pp. 1510-1518, 2005.

[10] V. Terzija *et al.*, "Wide-area monitoring, protection, and control of future electric power networks," *Proceedings of the IEEE,* vol. 99, no. 1, pp. 80-93, 2010.

[11] N. Senroy, "Generator coherency using the Hilbert–Huang transform," *IEEE Transactions on Power Systems,* vol. 23, no. 4, pp. 1701-1708, 2008.

[12] G. Rogers, *Power system oscillations*. Springer Science & Business Media, 2012.

[13] J. H. Chow, *Time-scale modeling of dynamic networks with applications to power systems*. Springer, 1982.

[14] S. Yusof, G. Rogers, and R. Alden, "Slow coherency based network partitioning including load buses," *IEEE Transactions on Power Systems,* vol. 8, no. 3, pp. 1375-1382, 1993.

[15] I. Tyuryukanov, M. Popov, M. A. van der Meijden, and V. Terzija, "Slow Coherency Identification and Power System Dynamic Model Reduction by Using Orthogonal Structure of Electromechanical Eigenvectors," *IEEE Transactions on Power Systems,* vol. 36, no. 2, pp. 1482-1492, 2020.

[16] X. Du, Y. Zhang, Q. Li, Y. Xiong, X. Yu, and X. Zhang, "New theory of extended coherency for power system based on method of coherency in differential geometry," in *2011 Asia-Pacific Power and Energy Engineering Conference*, 2011: IEEE, pp. 1-6.

[17] C. Li, J. Xu, and C. Zhao, "A coherency-based equivalence method for MMC inverters using virtual synchronous generator control," *IEEE Transactions on Power Delivery,* vol. 31, no. 3, pp. 1369-1378, 2015.

[18] B. Nun, M. F. Umar, A. Karaki, M. B. Shadmand, S. Bayhan, and H. Abu-Rub, "Rank-based Predictive Control for Community Microgrids with Dynamic Topology and Multiple Points of Common Coupling," *IEEE Journal of Emerging and Selected Topics in Industrial Electronics,* 2021.

[19] B. Nun, M. F. Umar, and M. B. Shadmand, "Enabling Resilient Community Microgrids with Multiple Points of Common Coupling via a Rank-Based Model Predictive Control Framework," in *2021 IEEE Applied Power Electronics Conference and Exposition (APEC)*, 2021: IEEE, pp. 2686-2691.

[20] M. F. Umar *et al.*, "Single-Phase Grid-Interactive Inverter with Resonance Suppression based on Adaptive Predictive Control in Weak Grid Condition," *IEEE Journal of Emerging and Selected Topics in Industrial Electronics,* 2021.